Translation in a Box:
Orthogonal Evolution in the *Saccharomyces cerevisiae* Mitochondrion

Brooke Rothschild-Mancinelli[1,2], Claudia Alvarez-Carreño[1,2], Wenying Guo[3], Chieri Ito[1,2], Alex Costa[3], Anton S. Petrov[1,2], Kirill Lobachev[3]* and Loren Dean Williams[1,2]*

[1]NASA Center for the Origin of Life, Georgia Institute of Technology, Atlanta, GA 30332-0400, USA

[2]School of Chemistry and Biochemistry, Georgia Institute of Technology, 901 Atlantic Dr, Atlanta, GA 30332, USA

[3]School of Biological Sciences, Georgia Institute of Technology, 901 Atlantic Dr, Atlanta, GA 30332, USA

* Corresponding authors:
Loren Dean Williams
Email: loren.williams@chemistry.gatech.edu
Kirill Lobachev
Email: kirill.lobachev@biology.gatech.edu

Preprint Servers: This manuscript was deposited as a preprint to bioRxiv under a CC-BY-NC 4.0 International license.

Classification: Synthetic Biology

Keywords: Orthogonal ribosome, translation

Abstract

The synthesis capabilities of the translation system (TS) provide engineering and directed evolution potential as well as a system for generating novel polymers. Orthogonal translation systems offer a parallel platform for translation engineering, enabling primary and secondary translation systems to operate independently without interfering with each other. However, current translation platforms for engineering lack complete orthogonality between the primary and secondary systems. Using a combination of indirect modifications through antibiotics, truncations of mito-rProteins mL50 and uL23, and replacement of mito-rProtein uL2, we develop and test the mitochondrial translation system in *Saccharomyces cerevisiae* as a fully orthogonal platform for *in vivo* directed evolution of translation. Our results show that continuous, comprehensive, creative, directed-evolution of a fully orthogonal TS *in vivo* appears to be a useful approach for technical control of the TS. This study emphasizes the power of system-wide evolutionary approaches over rational design. Evolution is creative and non-linear and can find unexpected solutions to problems.

Significance

All life operates on the central dogma, information flows from DNA to mRNA to protein. The translation system decodes mRNA and produces proteins. Engineering and evolving the translation system permits full technical control over this process and could lead to the generation of novel polymers. Here we explore the mitochondrial translation system in the budding yeast *Saccharomyces cerevisiae* for directed evolution of translation. We modify and evolve the translation system both directly and indirectly using antibiotics and gene editing tools and then measure resulting functionality. Our results show this secondary translation system inside *S. cerevisiae* mitochondria can be used as an approach for translation engineering.

Main text

Introduction

The translation system (TS) lies at the core of life processes, polymerizing amino acids into coded proteins using mRNAs as templates (1-3). The ability to re-engineer or creatively evolve the TS could lead to revolutionary advances in chemical and synthetic biology as well as in our understanding of principles underlying biology (4). Full technical control over the TS would allow us to expand the sidechain inventory of biopolymers and shift backbones into new chemical spaces (5,6). Functionalized proteins and genetically encoded polymers beyond biopolymers would lead to revolutionary tools in catalysis, therapeutics and materials.

Unfortunately, the TS is difficult to manipulate. The TS is tightly linked to transcription and other complex processes and is more resistant to change over evolution than any other aspect of biology (7-9). Many changes to the TS render it nonfunctional and are lethal, and the combinatorial space of random mutations is immense. Strategies to overcome these constraints are crucial for unlocking the full technological potential of the translation system.

Introduction of a second, completely independent (orthogonal) TS can release some constraints on TS engineering *in vivo*. A primary TS can be used produce proteins to maintain viability, allowing radical changes in a secondary TS (10,11). Partially orthogonal dual systems have been developed that enforce some separation between primary and secondary TS's. Secondary mRNAs and small subunit (SSU) rRNAs use manipulated Shine-Dalgarno/anti-Shine-Dalgarno sequences to enforce orthogonality (11). These secondary mRNA/SSU RNA systems have been extended to include large subunit (LSU) RNAs by covalently coupling SSU and LSU rRNAs (12-14). In addition, codons can be repurposed so that engineered aminoacyl-tRNA synthetase/cognate tRNA pairs direct incorporation of unnatural amino acids (6,15).

Optimally, the secondary TS would be entirely *orthogonal* to the primary TS, using distinct rRNAs, rProteins, ribosomal subunits, translation factors, aminoacyl tRNA synthetases, tRNAs, and mRNAs. With fully orthogonal dual TS's, changes in the secondary TS would not impact the primary TS, enabling continuous, comprehensive, creative, directed-evolution of the TS *in vivo*. In each of the dual systems described above, rProteins, translation factors, and most tRNAs and aminoacyl tRNA synthetases are shared between the primary and secondary systems. To our knowledge there are no previous descriptions of the use of fully orthogonal systems for TS evolution.

Our approach to TS orthogonality here leverages the mitochondrion of *Saccharomyces cerevisiae*. The *S. cerevisiae* mitochondrial translation system is fully orthogonal to the cytosolic translation system. Mito-rRNAs, mito-rProteins, mito-tRNAs, mito-aminoacyl tRNA synthetases, and mito-translation factors are distinct from, physically separated from, and functionally independent of their cytosolic counterparts. Further, the dependence of *S. cerevisiae* survival on mitochondrial translation can be toggled on and off. By changing the carbon source in the growth media, *S. cerevisiae* survive by either fermentation or respiration (16-18). Growth on glucose

(fermentation) is independent of mitochondrial translation while growth on glycerol (respiration) requires mitochondrial translation.

Here, the *S. cerevisiae* mitochondrial translation system was subjected to various stresses including antibiotics, mutagenesis of mito-rProtein, or wholesale replacement of mito-rProteins. Directed evolution of these stressed systems was facilitated by controlled shifts between fermentation and respiration. A glucose medium (YPD) is permissive (not requiring mito-translation), and a glycerol medium (YPG) is non-permissive (requiring mito-translation). Suppression of mito-translation disfunction is indicated by growth in non-permissive conditions and is quantified here by flow cytometry using a reporter strain in which mitochondrial translation produces mito-sfGFP (superfolder Green Fluorescence Protein) (19). If mito-translation is inhibited, mutations can be accumulated under permissive conditions. Selection of suppressor mutants (those that suppress the non-functional phenotype) is achieved under non-permissive conditions. We used well-developed tools of *S. cerevisiae* genetics and characterized mutations by whole genome sequencing.

Results

Evolution of antibiotic resistance

As proof-of-concept that one can conduct directed evolution of the *S. cerevisiae* mito-TS by the system used here, we evaluated regain of mito-translation after it was blocked by well-characterized small molecules. We evolved resistance to the mito-ribosome-targeting antibiotics chloramphenicol and erythromycin and accumulated mutations in the MOY1355 strain (Materials and Methods). We compared the accumulated mutations to previous mutations known to confer resistance to bacterial and mito-ribosomes.

Resistance to chloramphenicol. Chloramphenicol binds to the peptidyl transferase centers of bacterial and mito-ribosomes and prevents peptide bond formation (20). Chloramphenicol does not target cytosolic ribosomes of eukaryotes such as *S. cerevisiae* (21). Selective inhibition of mito-ribosomes was confirmed here by chloramphenicol dependent growth of the wild-type strain on non-permissive media (Figure 1a). Lack of inhibition of cytosolic ribosomes by chloramphenicol was confirmed by chloramphenicol independent growth on permissive media (Supplementary Figure 1).

We evolved resistance to chloramphenicol (Cam^R) in MOY1355 through growth in the permissive medium, to accumulate mutations, followed by growth on non-permissive media containing chloramphenicol to select for suppressors (Figure 1a). Sequencing revealed that Cam^R strains contain mutation A2769C, a SNP in the peptidyl transferase center (PTC) of the SSU rRNA of the mito-ribosome (Supplementary Table 1; Figure 1b). This SNP (referred to as A2503C) was previously shown to confer resistance of mito-ribosomes and bacterial ribosomes to chloramphenicol (22). Mito-translation function of the Cam^R strain in non-permissive media is greater than that of wild-type MOY1355 ($p < 0.0001$). Cell growth and mito-translational function of Cam^R mutants were maintained in non-permissive media in the presence of chloramphenicol, albeit at slightly reduced levels. Mito-translation of MOY1355 was inhibited in non-permissive media in the presence of chloramphenicol, as indicated by lack of mito-sfGFP fluorescence; the fluorescence intensity is equivalent to that of the non-fluorescent control (Figure 1c).

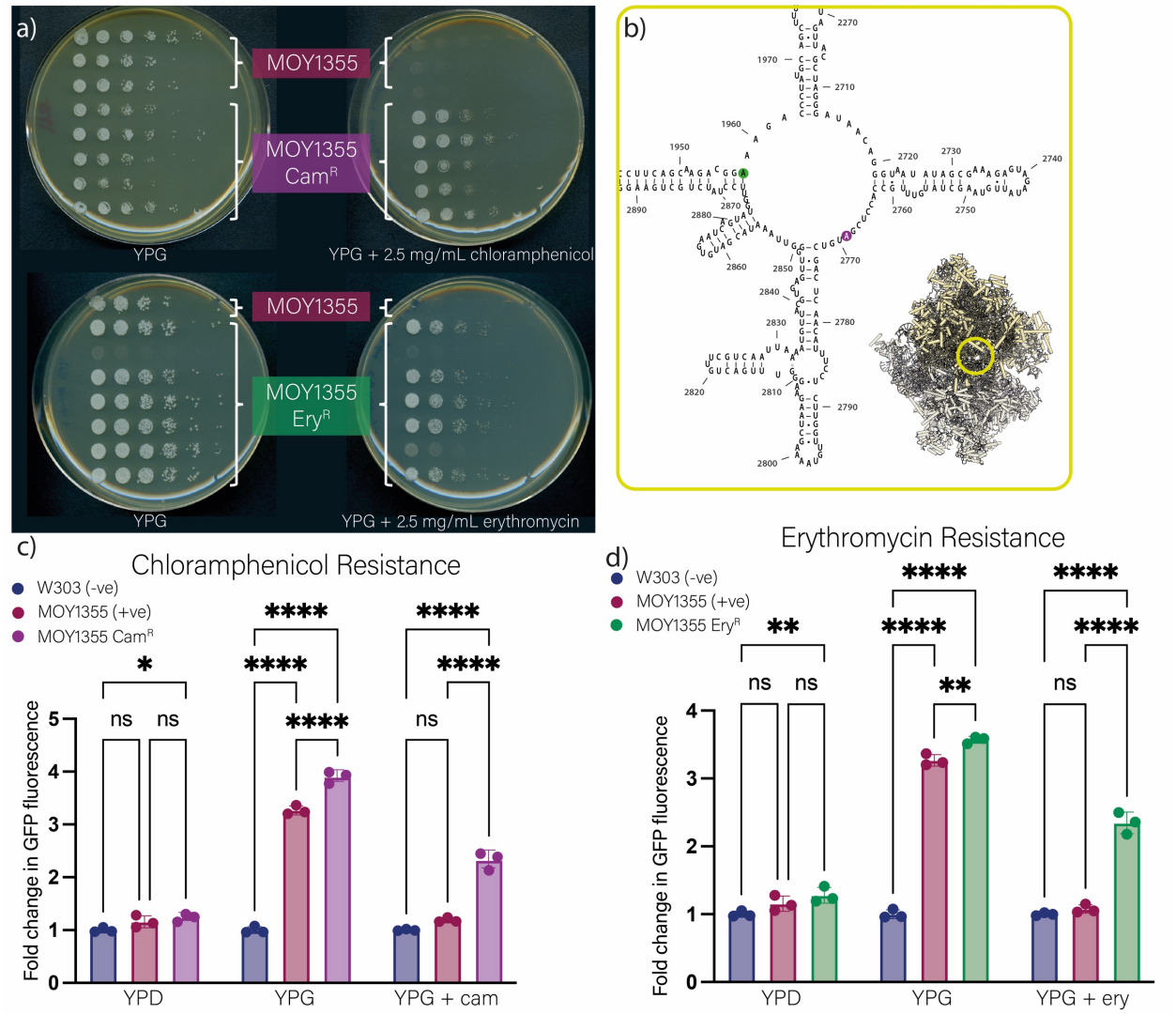

Figure 1. Mutations in mito-rRNA confer resistance to chloramphenicol and erythromycin. a) Growth of MOY1355, Cam^R, and Ery^R on non-permissive (YPG), non-permissive + 2.5 mg/mL chloramphenicol, and non-permissive + 2.5 mg/mL erythromycin media. b) The location of the A2769C (A2503C) SNP in the 21S rRNA of the mito-ribosome in the Cam^R strain is indicated in the the 3D and 2D structure of the ribosome (PDB code 5MRC). c) and d) Function of the mito-translation system assayed by flow cytometry after growth in permissive (YPD), non-permissive (YPG), and non-permissive + antibiotics (YPG + 2.5 mg/mL chloramphenicol or erythromycin). W303 (blue) is the non-fluorescent negative control, MOY1355 (maroon) is the wild-type (WT) fluorescent positive control derived from W303 and the Cam^R strain (purple) Ery^R strain (green) are derived from MOY1355. Mean fluorescence intensity values were divided over W303 for the same experiment and media conditions to determine fold change over background (N = 10,000). ns = $p > 0.05$, * = $p \leq 0.05$, ** = $p \leq 0.01$, *** = $p \leq 0.001$, *** = $p \leq 0.0001$.

Resistance to erythromycin. Erythromycin obstructs the exit tunnel of bacterial and mito-ribosomes but not cytosolic ribosomes of eukaryotes (20). As with chloramphenicol, erythromycin selectively inhibits mito-ribosomal function in *S. cerevisiae* (Supplementary Figure 2). We evolved resistance to erythromycin (Ery^R) in MOY1355 via growth in permissive media to accumulate mutations, followed by selection in non-permissive media containing erythromycin. Resistant mutants (Ery^R) sustained erythromycin-independent growth in non-permissive media (Figure 1a). Wild-type MOY1355 grew in non-permissive media, only in the absence of

erythromycin (Figure 1a). Sequencing of Ery^R isolates revealed a A1958G SNP in the LSU mito-rRNA (Supplementary Table 1; Figure 1b). This SNP has been shown previously to confer resistance to erythromycin (referred to as A2508G) (23). Florescence intensity suggests that function of mito-translation of the Ery^R strain in non-permissive media is greater than that of wild-type MOY1355 ($p = 0.0018$). Cell growth and mito-ribosomal function of Ery^R mutants were maintained in non-permissive media in the presence of erythromycin, albeit at slightly reduced levels. MOY1355 did not grow on non-permissive media in the presence of erythromycin; mito-translation function was similar to that of the non-fluorescent control (Figure 1d).

Mito-rProtein perturbations

The results with antibiotics (above) demonstrate that directed evolution of the mito-ribosome is a viable approach that can give interpretable mutations. Thus, we investigated evolutionary adaptation to changes in mito-rProteins. The orthogonality of the cytosolic and mito-translation systems allows targeted perturbation of mito-rProteins without affecting cytosolic rProteins. We made various edits to sequences of mito-rProteins. Edited mito-rProteins are incorporated into the mito-ribosome but not the cytosolic ribosome. We evolved and sequenced suppressor strains with recovered mito-translational functionality.

Our goal here was to manipulate one of the central and critical structures of the TS – the exit tunnel. Technological control over exit tunnel geometry appears to be required for production of novel backbones (5). The canonical ribosomal exit tunnel is diverted in the *S. cerevisiae* mito-ribosomes (24,25) in part by an extension of mito-uL23 as well as by association recruitment of mL50 (26). As a proof-of-concept we used directed evolution to recover function of mito-ribosomes with perturbations of the exit tunnel.

Truncated Mito-rProtein mL50. $mL50_{1\text{-}264}$ (1-264 indicates the length of the native protein) is an integral part of the *S. cerevisiae* mito-exit tunnel (Figure 2a). $mL50_{1\text{-}264}$ was truncated here by the removal of part of the C-terminal α-helix (aa 250-264) to create $mL50_{1\text{-}249}$ within MOY1355. It was anticipated that $mL50_{1\text{-}249}$ would significantly impair mito-translation. Indeed, the $mL50_{1\text{-}249}$ strain showed decreased mito-ribosomal function compared to MOY1355. Mito-function decreased from 3.3-fold over background to 2.3-fold over background as suggested by mito-sfGFP fluorescence ($p < 0.0196$; Figure 2c).

After directed Adaptive Laboratory Evolution (ALE) (27) over 100 generations of the $mL50_{1\text{-}249}$ strain, mito-translation function was recovered through spontaneous accumulation of mutations. Our ALE scheme selected for rapid growth of the $mL50_{1\text{-}249}$ strain in non-permissive media over 100 generations as mito-translation is critical for growth in those conditions (Figure 2c). After 100 generations, three colonies from three independent evolution cultures were isolated. Mito-translation was assayed in each in non-permissive media by fluorescence of mito-sfGFP per cell. Mito-translation function in all three isolates appeared, by these measures, to be equivalent to MOY1355 (Figure 2c). An alternative evolution scheme of oscillating between permissive and non-permissive media was tested, but showed a less consistent increase in mito-ribosome function (Supplementary Figure 3).

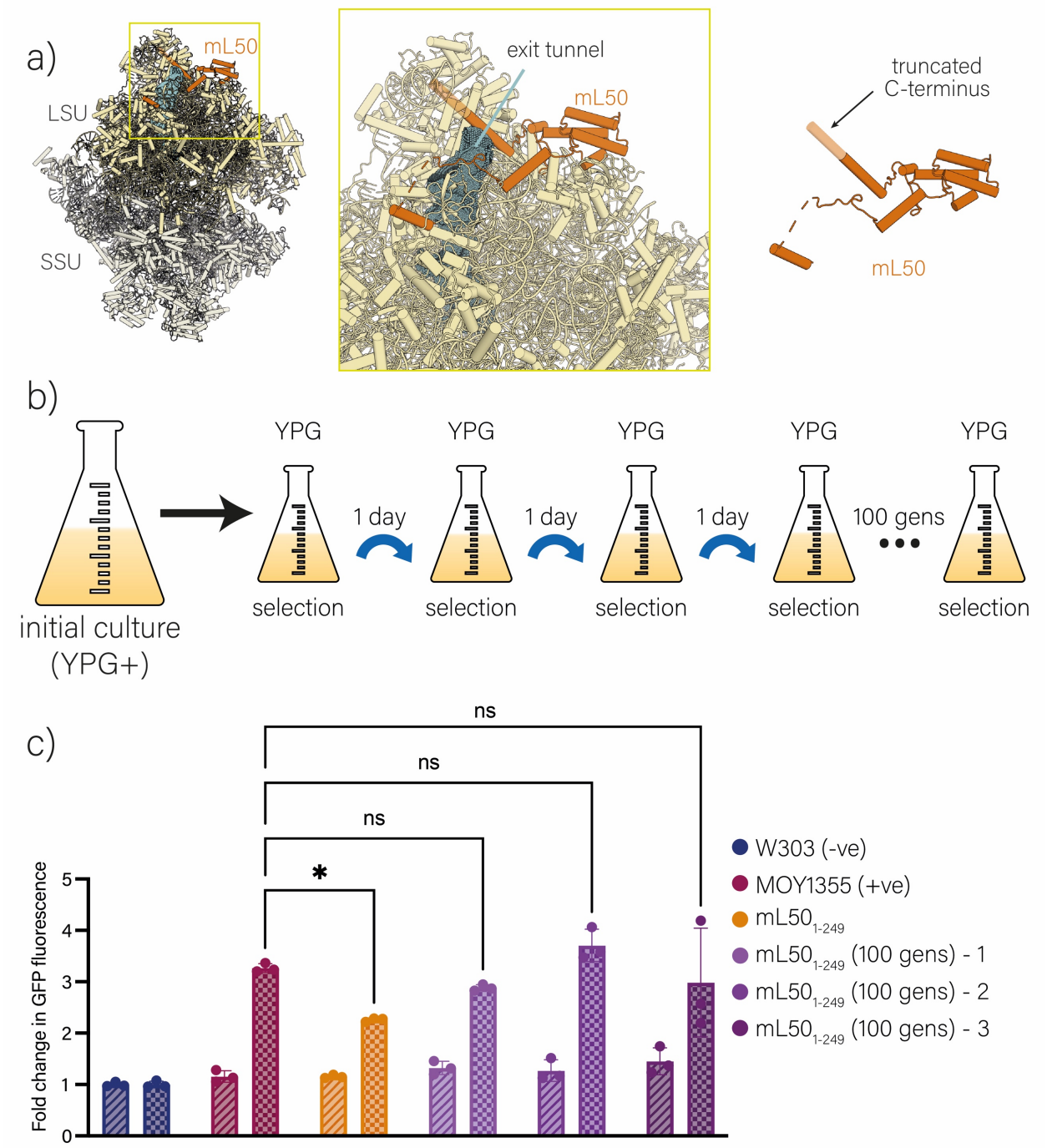

Figure 2. Decreased function of mL50$_{1-249}$ can be recovered via ALE. a) Location of the mL50 truncation in the mito-ribosome (PDB code 5MRC). mL50 is shown in orange. b) the ALE evolution scheme used to increase mito-translation function over 100 generations in non-permissive (YPG) media only. c) Function of the mito-translation system assayed on the flow cytometer after growth in permissive (YPD; diagonal stripes) and non-permissive (YPG; checked pattern) media. W303 (blue) is the non-fluorescent negative control, MOY1355 (maroon) is the WT fluorescent positive control derived from W303 and mL50$_{1-249}$ (orange) is the initial truncated strain with its evolved counterparts in shades of purple. Mean fluorescence intensity values were divided over W303 for the same experiment and media conditions to determine fold change over background (N = 10,000). ns = $p > 0.05$, * = $p \leq 0.05$, ** = $p \leq 0.01$, *** = $p \leq 0.001$, *** = $p \leq 0.0001$.

Isolation of suppressors for truncated Mito-rProtein uL23. uL23 is a universal rProtein located adjacent to the exit tunnel, with homologs across the tree of life. uL23 is essential for translation, and impacts nascent protein folding (28). The cytosolic and mito-uL23 rProteins are nuclear encoded. As an architectural component of the diverted exit tunnel of the *S. cerevisiae* mito-ribosome (Figure 3a) (26), changes in mito-uL23 are expected to impact mito-translation.

We edited the sequence of mito-uL23 by removing the C-terminal α-helix. Mito-uL23$_{1\text{-}261}$ (1-261 indicates the length of the native mito-rProtein) was truncated in MOY1355 by the removal amino acids 225-261 to create mito-uL23$_{1\text{-}224}$. The results suggest that this edit shuts down mito-translation. No growth of the mito-uL23$_{1\text{-}224}$ strain was observed on non-permissive media (Figure 3b). Fluorescence of mito-sfGFP in the mito-uL23$_{1\text{-}224}$ strain measured via flow cytometry was equivalent to in the non-fluorescent control (Figure 3c).

We re-evolved mito-translation functionality in the mito-uL23$_{1\text{-}224}$ strain. As with antibiotic resistance evolution, mutations were accumulated during growth in permissive media followed by selection in non-permissive media. Four suppressor strains of the mito-uL23$_{1\text{-}224}$ phenotype, that grew on non-permissive media, were identified (Figure 3b). Sequencing revealed all four suppressors had a S39I change in protein Rrg9 and truncations in protein AI1 that were not present in mito-uL23$_{1\text{-}224}$ pre-evolution strain (Figure 4a). While the function of Rrg9 is unknown, it localizes in the mitochondrion and interacts with components of the mito-translation system (Figure 4b) (29-32). Deletion of *RRG9* renders *S. cerevisiae* unable to respire (33). The mito-translation function of the four mito-uL23$_{1\text{-}224}$ suppressors in non-permissive media remained low, with only Suppressor 1 having mito-translation function above W303 background fluorescence levels with a 1.6 fold increase ($p = 0.0027$).

The ALE method established with mL50$_{1\text{-}249}$, was used for directed evolution of the mito-uL23$_{1\text{-}224}$ strain. Over 100 generations, mito-translation function recovered through spontaneous accumulation of mutations. Three colonies were isolated from each of three independently evolved cultures and mito-translation was assayed in non-permissive media by growth rate on non-permissive media and by fluorescence of mito-sfGFP. Increased mito-translation function compared to the original suppressor was observed in most isolates (Figure 5b; supplementary Figure 4). We qualitatively assayed mitochondrial numbers using confocal microscopy to ensure increasing fluorescent values in evolved strains were due to an increase in mito-translation and not an increase in number of mitochondria. Images of MOY1355, mito-uL23$_{1\text{-}224}$, and suppressors showed consistent numbers of mitochondria (supplementary Figure 5).

Three of the four suppressors evolved over 100 generations acquired mutations in protein Mrx1. Mutations are R180I, W224S, and V199F (Figure 4a). This protein is known to associate with the mito-ribosome and other factors involved in mito-translation (Figure 4b) and Mrx1 knock-outs are respiration deficient and is therefore a potential part of the mito-translation system. Additional non-synonymous mutations were found in *MCK1*, *PUF6*, and *RTX3* (Figure 4a).

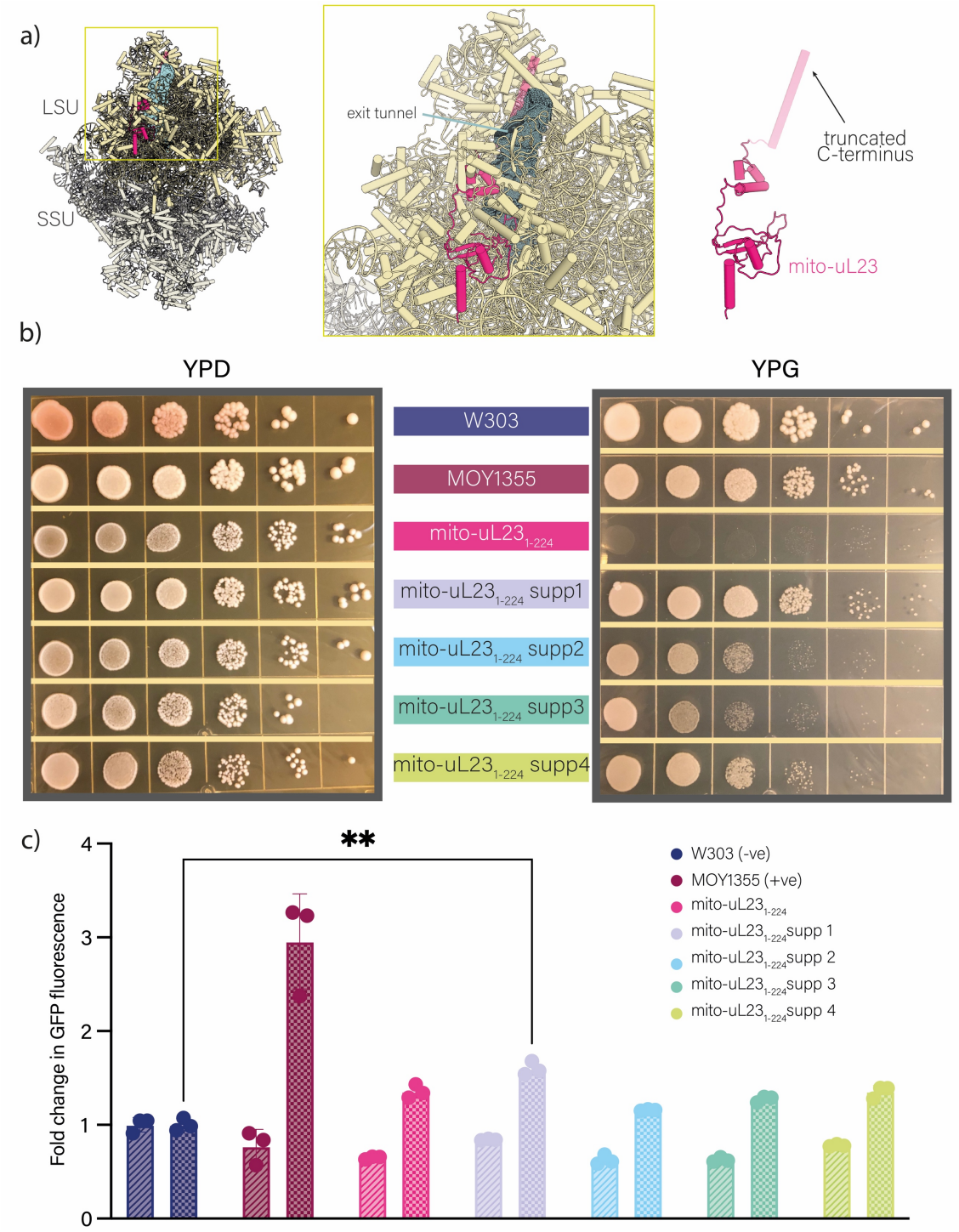

Figure 3. Mito-uL23$_{1\text{-}224}$ can recover mito-translation via evolution. a) Location of the mito-uL23 truncation in the mito-ribosome (PDB code 5MRC). mito-uL23 is shown in pink. (b) Growth of wild-type strains, mito-uL23$_{1\text{-}224}$, and the four suppressors on both permissive (YPD) and non-permissive (YPG) media. c) Function of the mito-translation system assayed in all strain in the flow cytometer after growth in permissive (YPD) and non-permissive (YPG) media. Permissive media is denoted with diagonal lines and non-permissive with checks Mean fluorescence intensity values were divided over W303 for the same experiment and media conditions to determine fold change over background (N = 10,000). ns = $p > 0.05$, * = $p \leq 0.05$, ** = $p \leq 0.01$, *** = $p \leq 0.001$, *** = $p \leq 0.0001$.

a)

	Chr	II			IV			V	XIII	XIV		XVI	Mito
	Gene name	*IRA1*	*NTC20*	*YBR220C*	*RXT3*	*PUF6*	*CMR1*	*MRX1*	*ALD2*	*MCK1*	*RRG9*	*KRE6*	*AI1*
mito-uL23$_{1-224}$			E44A	V296I									
supp 1	0 gen	○		V296I							S39I		AI1$_{1-754}$
	100 gen	○		V296I	E164			R180I			S39I		AI1$_{1-754}$
supp 2	0 gen			V296I			G118Q				S39I		AI1$_{1-754}$
	100 gen			V296I			G118Q	W224S			S39I		AI1$_{1-754}$
supp 3	0 gen			V296I						○	S39I		AI1$_{1-754}$
	100 gen			V296I		PUF6$_{1-331}$				W224S	S39I		AI1$_{1-754}$
supp 4	0 gen			V296I					○		S39I	Kre6$_{1-389}$	AI1$_{1-754}$
	100 gen			V296I				V199F	○		S39I	Kre6$_{1-389}$	AI1$_{1-754}$

b)

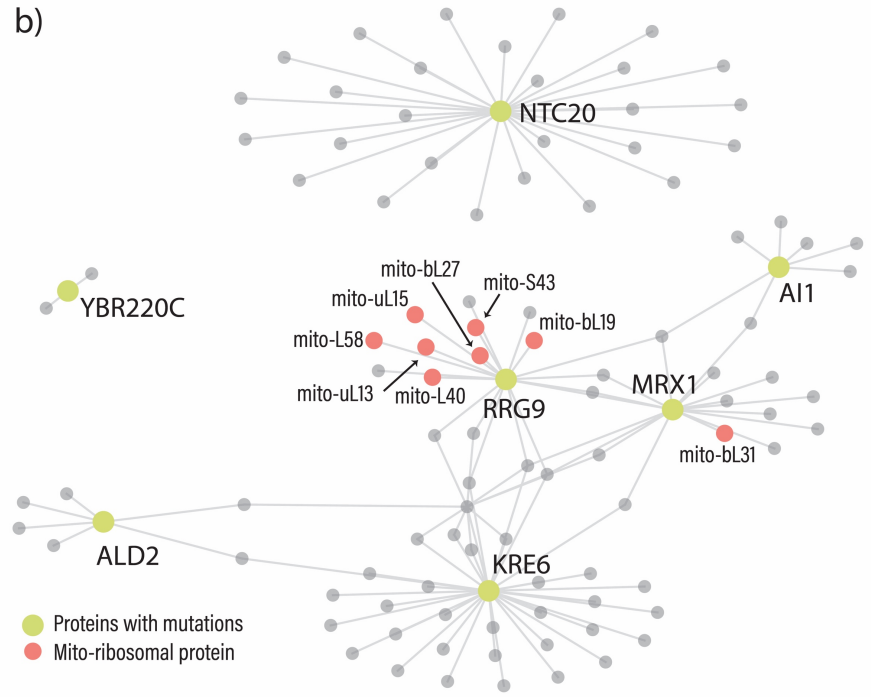

Figure 4. mito-uL23$^{1-224}$ suppressors. a) Mutations found in protein-coding genes in mito-uL23$_{1-224}$ and four suppressors. 0 gen: initial suppressor. 100 gen: suppressor strain after 100 generations. b) Map of protein interactions of the proteins presenting mutations in suppressor 4. Proteins are represented by nodes, and physical interactions curated by BioGRID (34) are represented by lines between nodes. Green nodes: mutated proteins in suppressor 4. Pink: ribosomal proteins and other proteins related to translation. Blue: mitochondrial proteins.

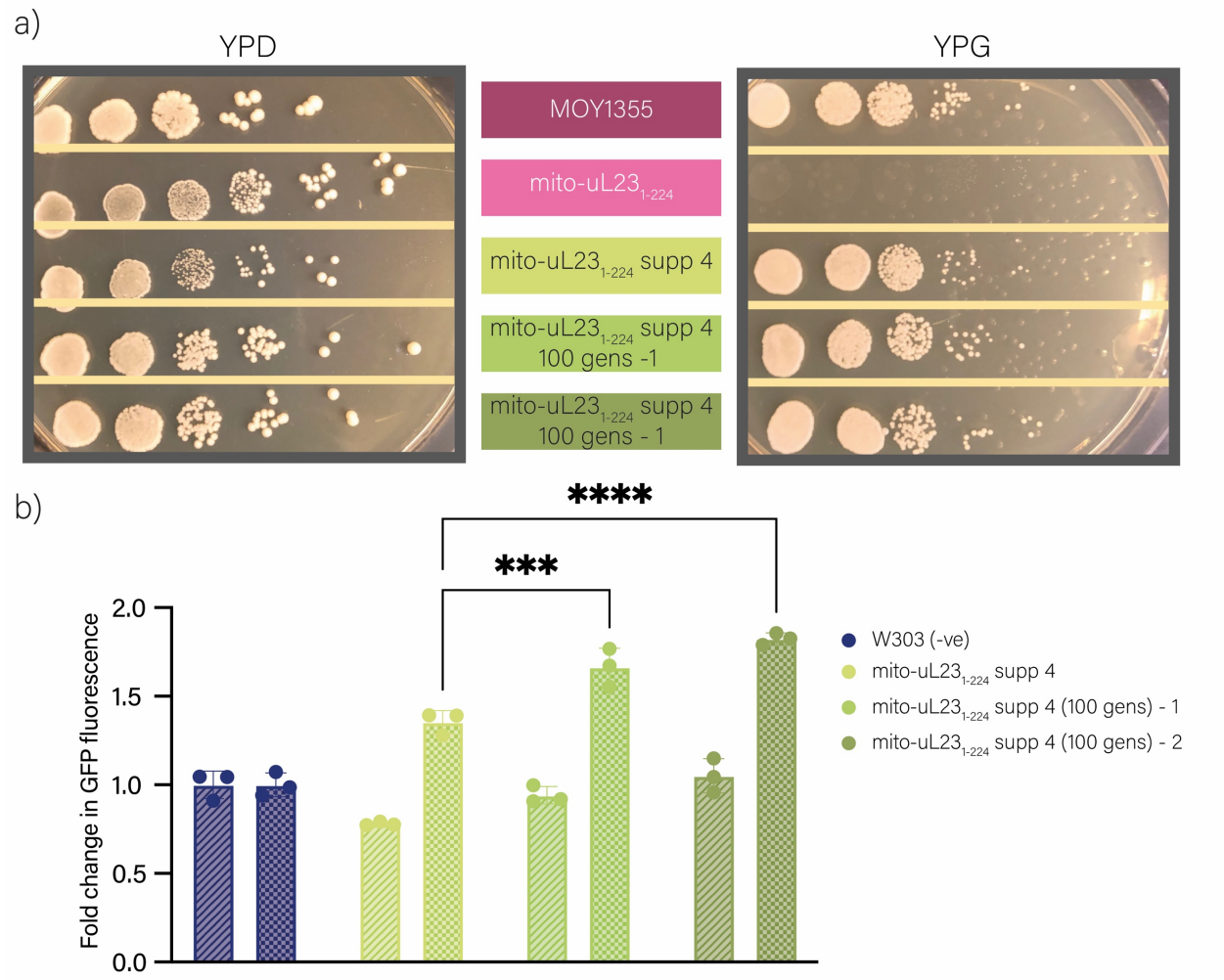

Figure 5. Mito-uL23$_{1-224}$ Suppressor 4 function increases after 100 generations of ALE in non-permissive conditions. a) Growth of wild-type strains, mito-uL23$_{1-224}$, suppressor 4 and suppressor 4 after 100 generations on both permissive (YPD) and non-permissive (YPG) media. b) Function of the mito-translation system assayed in all strains in the flow cytometer after growth in permissive (YPD) and non-permissive (YPG) media. Permissive media is denoted with diagonal lines and non-permissive with checks. Mean fluorescence intensity values were divided over W303 for the same experiment and media conditions to determine fold change over background (N = 10,000). ns = $p > 0.05$, * = $p \leq 0.05$, ** = $p \leq 0.01$, *** = $p \leq 0.001$, *** = $p \leq 0.0001$.

Replacement of mito-rProteins

The *S. cerevisiae* mito-translation system can be used as a platform for replacing ribosomal proteins with homologs from other species, and/or with ancestral reconstructions. We used rProtein uL2 to test the ability of yeast to survive and respond to global and local modifications to mito-uL2. uL2 is a universal ribosomal protein that is essential for peptidyl transfer (35). To measure the impact of a global but minimal change, we replaced one mito-uL2 gene (*RML2)* with

another, while holding the of amino acid sequence constant. We substituted the *S. cerevisiae* mito-uL2 sequence with a sequence optimized for cytosolic expression in *S. cerevisiae.* The resulting altered *RML2* encoded the native mitochondrial amino acid sequence with 78% nucleotide identity to the WT gene (supplementary Table 2). The resulting strain (mito-uL2$_{codon-optimized}$) grew more slowly than wild-type in non-permissive media (Figure 6c) and had slightly reduced mito-ribosomal function compared to MOY1355 when assayed by mito-sfGFP, from 3.0-fold over background to 2.5-fold over background ($p = 0.0279$; Figure 6d).

Comparisons of experimental structures of mito-ribosomes reveal that the C-terminus of mito-uL2 is structurally variable over phylogeny, making this region of mito-uL2 an interesting target for modification. We replaced the 44 C-terminal amino acids of *S. cerevisiae* mito-uL2 with 44 C-terminal amino acids of the *Schizosaccharomyces pombe* homolog of mito-uL2. This substitution changed 29 of 44 amino acids of the C-terminal tail (Figure 6b). The resulting growth was comparable in non-permissive media to the codon-optimized mito-uL2, although mito-translation function decreased from 2.5-fold to 1.9-fold over background ($p = 0.0065$).

Lastly, we inferred the amino acid sequence of an ancestral mito-uL2 from a multiple-sequence alignment of uL2 and mito-uL2 homologs across the tree of life. We replaced the 44 C-terminal amino acids of the *S. cerevisiae* mito-uL2 with the C-terminus of the inferred ancestral reconstruction of the mitochondrial common ancestor with a total of 27 amino acids changed and 3 deleted (mito-uL2$_{mitochondrial\ node}$; Figure 6b). In non-permissive conditions, this modification reduced growth (Figure 6c). Mito-uL2$_{mitochondrial\ node}$ could grow on non-permissive media, although mito-translation is reduced (Figure 6d). These results are consistent with the divergence in amino acid properties in the replaced segment of mito-uL2 (Figure 6b).

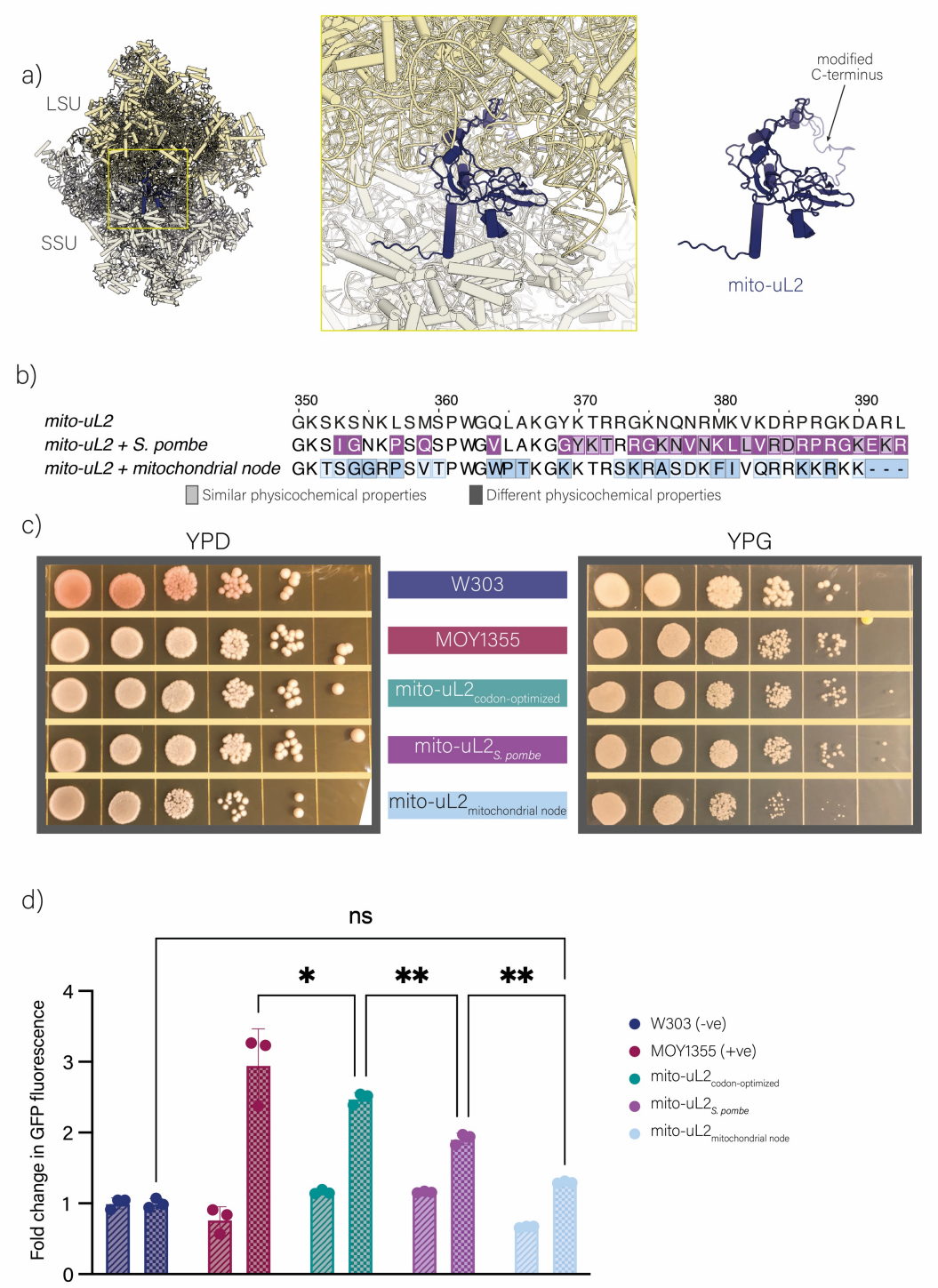

Figure 6. Modifications to mito-uL2 decrease mito-translation. Location of the mito-uL2 truncation in the mito-ribosome (PDB code 5MRC). mito-uL2 is shown in blue. c) Growth of wild-type strains, mito-uL2$_{\text{codon-optimized}}$, mito-uL2$_{S.\ pombe}$, and mito-uL2$_{\text{mitochondrial node}}$ in both permissive (YPD) and non-permissive (YPG) media. b) Function of the mito-translation system assayed in all strains in the flow cytometer after growth in permissive (YPD) and non-permissive (YPG) media. Permissive media is denoted with diagonal lines and non-permissive with checks. Mean fluorescence intensity values were divided over W303 for the same experiment and media conditions to determine fold change over background (N = 10,000). ns = $p > 0.05$, * = $p \leq 0.05$, ** = $p \leq 0.01$, *** = $p \leq 0.001$, *** = $p \leq 0.0001$.

Discussion

Nature has offered us dual fully orthogonal translation systems in *S. cerevisiae*. The primary TS is located in the cytosol and is descended from the TS of an archaeon (36). The secondary TS is located in the mitochondrion and is descended from the TS of an α-proteobacterium (37,38). In *S. cerevisiae,* the primary TS is universally necessary for survival and the secondary TS is conditionally necessary for survival. Genes encoding mito-translation factors, mito aminoacyl-tRNA synthetase - (aaRS's and most mito-rProteins are located in the nuclear genome; these proteins are directed to mitochondria by targeting sequences (mitochondria localization signal) (39). Genes encoding mito-rRNAs and mito-tRNAs are located in the mitochondrial genome, which also encodes seven integral membrane proteins required for respiration and one soluble mito-rProtein (mito-uS3) (39).

The orthogonality of the dual TS's of *S. cerevisiae*, and the conditional dependence of one of them, offers the possibility of continuous, simultaneous directed evolution of all contributing components of a fully functioning TS *in vivo*. The combined results here indicate that perturbations of the mito-TS can cause repeatable and generally interpretable compensatory changes over evolution to the mito-TS components.

The functionality of the mito-TS was quantitated here via flow cytometry, growth on non-permissive media and sequencing. The fluorescence intensity of mito-sfGFP was measured to indicate the relative functionality of the mito-TS. Microscopy results here are consistent with a previous demonstration of containment of mito-sfGFP within mitochondria and the lack of change in the number of mitochondria over the course of our experiments (Supplementary Figure 5). Fluorescence of mito-sfGFP indicates that the unusual geometry of the *S. cerevisiae* mito-TS tunnel (24) does not prevent folding of soluble proteins.

We validated the general utility of the *S. cerevisiae* mito-TS in directed evolution experiments using well-characterized mito-ribosome-targeting inhibitors, chloramphenicol and erythromycin. The SNPs to confer resistance to these antibiotics had been previously identified (22,23) but resulting mito-translation had not been quantified. Sequencing, flow cytometry and growth on non-permissive media indicate full recovery of TS function is achieved by mutations of the LSU mito-rRNA.

We investigated the evolutionary response of the mito-TS to changes in mito-rProteins. We re-evolved full mito-TS functionality after truncation of mL50 or mito-uL23. Suppressors of mito-uL23 truncation phenotype, with recovered function, consistently show mutations in mito-proteins Rrg9 and Mrx1. These proteins are known to interact with the mito-ribosome (32) and cause respiratory deficiency when absent (33,40,41) but have not previously been ascribed function. The results here do not define the function of Rrg9 or Mrx1 but allow to propose that

Rrg9 and Mrx1 interact with the mito-TS and have critical role in its function. It was not possible to predict with current knowledge that mutations in *RRG9* and *MRX1* would recover mito-TS function.

We probed the effect of whole replacement of universal rProtein mito-uL2 on the mito-TS. We substituted the native *RML2* gene first with a codon-optimized sequence and then further replaced the C-terminal tail with sequences from *S. pombe* and the mitochondrion in the last universal eukaryotic ancestor. To our knowledge *in vivo* ancestral reconstructions of parts of the ribosome have never been used before. These modifications showed reduced function and could be further evolved as with mito-uL23 to start to push the ribosome back in time.

There are some disadvantages to the mito-TS as a target of directed evolution. mito-rRNAs and mito-tRNAs are encoded on the mito-genome, and are difficult to manipulate by conventional techniques of molecular biology. However, the mitochondrial genome can be manipulated using biolistic bombardment and homologous recombination (42). Less precise approaches to mito-genome engineering use base editors, like deaminases, engineered to contain mitochondrial targeting signals (43). The other disadvantage to the mito-TS is the propensity for *S. cerevisiae* to lose mito-genomes when cells lack specific proteins associated with mitochondrial transcription and translation (e.g. mL54, mS35, Mtf1) (44) (33). The upregulation of *RNR1* has been shown to decrease mito-genome loss in wild-type *S. cerevisiae* (45).

The mito-TS could also be used for incorporation of non-canonical amino acids as the aaRS's are encoded on the nuclear genome. The *E. coli* tyrosine aaRS has been shown to charge specifically the *S. cerevisiae* mitochondrial $tRNA^{Tyr}$. Alterations to the *E. coli* $aaRS^{Tyr}$ has been shown to incorporate photoaffinity probes, bioconjugation handles, and a nonhydrolyzable mimic of phosphotyrosine (46). Furthermore, there are codons not in use in the mito-genome, including the CGN family of arginine codons (47), offering an opportunity for genetic code expansion that will not affect native mito-translation.

Full technical control of the TS will allow expansion of the sidechain inventory of biopolymers and transformation of backbones into new chemical spaces. These advances will require that we overcome evolutionary forces that have held the TS essentially fixed for billions of years. Advances require transformation of catalytic competencies of the PTC and aaRS and of delivery/transport functionality of the exit tunnel (28,48-50). A host of factors including rRNAs, tRNAs, translation factors, aaRS's, and rProteins are directly involved in these processes and many other factors are indirectly involved. Continuous, comprehensive, creative, directed-evolution of a fully orthogonal TS *in vivo* is a useful approach for technical control of the TS. The work here indicates the power of system-wide evolutionary approaches over rational design. As demonstrated by our experiments thus far, evolution is creative and non-linear and can find unexpected solutions to problems.

Materials and Methods

Strains, plasmids and oligonucleotides

The W303 strain was a gift from Dr. Thomas Petes (Duke University). The MOY1355 strain (Mat α ade2-1 his3-11,15 trp1-1 leu2-3,112 ura3-1, sfGFPm::cox2, COX2) (19) was a gift from Dr. Martin Ott (Stockholm University). Other strains were derivatives of MOY1355. Freshly thawed yeast strains were streaked onto YPG (if YPG+) or YPD (if YPG-) and grown at 30 °C in the presence of atmospheric O_2. Permissive media (YPD) is 1% yeast extract, 2% peptone, 2% glucose and non-permissive (YPG) is 1% yeast extract, 2% peptone, 3% [v/v] glycerol). Uracil dropout, YPD + G418 (0.3 mg/mL) and 5-fluoroorotic acid were used for the development of strains. Strains were constructed either with the *kanMX* marker (mL50 and uL23 perturbations) or CRISPR (uL2 replacements). *kanMX* and *URA3* marker truncations were made by amplifying the *kanMX* region of pKL55 or *URA3* of pFL34 using primers with 40 bp homology to the gene sequence for *mrp20* and *mrpl13*. The uL2 strains were created using CRISPR/Cas9 to replace the existing *RML2* gene with a synthesized gene.

CRISPR

The gRNAs were designed using the CRISPR Design Tool in Benchling and assembled into the CRISPR backbone (Addgene plasmid 198866) using Golden Gate assembly designed in Benchling. The assembled plasmids were transformed into *E. coli* dh5α and grown overnight on LB + 50 µg/mL spectinomycin at 37 ºC. Non-fluorescent colonies were picked and grown overnight in liquid LB + 50 µg/mL spectinomycin and miniprepped using the Qiagen miniprep kit (Cat. No. / ID: 27104). Plasmid assembly was verified by sequencing (eurofins Genomics).

Yeast Transformation

To maintain the mito-genome in the transformation, cells were inoculated in 5 mL liquid YPG for the initial growth from colonies for 2 days, shaking at 200 rpm. The starter culture was back-diluted in 50 mL YPD to a final OD of ~0.15 and replaced in the incubator. The OD was monitored and when the culture reached an OD of 0.6-0.8 the cells were harvested at 2500 rpm for 5 min. The supernatant was decanted and the pellet resuspended in 20 mL autoclaved H_2O and spun once again. The supernatant was discarded again and the pellet resuspended in 400 µL H_2O. 150 µL of cell suspension was pipetted into a 1.5 mL Eppendorf and spun down for 30 seconds at 13,000 rpm in a tabletop centrifuge. The supernatant was discarded and the pellet was resuspended in 148 µL DNA mixture (for CRISPR: 200 ng CRISPR plasmid, 1000 ng donor DNA (NotI digest plasmid); for kanMX: 40µL gel-purified DNA, 108 µL H_2O) and 20 µL salmon sperm DNA (boiled for 5 min, chilled on ice for 3 min). First PEG (50%, MW 3350; 480 µL) was added and then 72 µL 1M LiAC. The mixture was vortexed and incubated at 30 ºC for 30 mins, transferred to 42 ºC for 15 mins then plated on SD complete lacking uracil (CRISPR and mL50) or on YPD. Ura+ transformants were grown for three days at 30 ºC. To select for drug resistance, cells grown on YPD for one day were replica-plated onto YPD + G418 (0.3 mg/mL) plates. Colonies were picked and insertions were verified using colony PCR with Phire Plant Direct PCR Master Mix (ThermoScientific, Catalog number: F160L) followed by sequence verification (eurofins Genomics).

Evolution

Yeast strains we evolved via spontaneous mutation accumulation for both antibiotic resistance and suppression of the YPG- phenotype of the uL23 truncation. Mutation accumulation was done by inoculating colonies in 5 mL YPD and incubating overnight with shaking at 200 rpm. The saturated culture was plated on 20 plates (200 µL per plate) of either YPG, YPG + erythromycin (2 mg/mL) or YPG + chloramphenicol (2.5 mg/mL). The plates were monitored for 2 weeks of incubation and colonies were picked as antibiotic resistant strains and suppressors. For strains exhibiting antibiotic resistance, rRNA was sequenced first (Eurofins Genomics) followed by whole genome sequencing (Psomagen).

The Adaptive Laboratory Evolution protocol was adapted from Espinosa, *et. al* (51). Colonies were picked from YPG plates and grown overnight in liquid YPG, shaking at 200 rpm. The OD was measured and the culture was back-diluted to OD 0.1 in YPG or YPD, depending on the evolution scheme. The OD measurement and back-dilution process was repeated daily in either YPG only or oscillating between YPD and YPG. Once each culture reached ~100 generations, the final culture was diluted in autoclaved H_2O and plated on YPG. Three colonies were picked from each evolution culture to use for further analysis.

In silico

Homology search

The multiple-sequence alignment (MSA) of uL2 sequences from 66 bacteria and 52 archaea representing a Sparse and Efficient Representation of Extant Biology (7) was retrieved from ProteoVision (52). Mitochondrial sequences of uL2m from five Jakobid species (53) (*Jakoba libera*, *Andalucia godoyi*, *Seculamonas ecuadoriensis*, *Jakoba bahamiensis*, and *Reclinomonas americana*) were added to the MSA of uL2 with MAFFT v7.490 (54). The final MSA containing archaeal, bacterial, and mitochondrial sequences displayed a block structure with universally conserved, archaea-specific, and bacteria/mitochondrial-specific blocks. The MSA was trimmed to the universal blocks with BMGE v1.12 (55) with default parameters.

Ancestral sequence reconstruction

A maximum likelihood tree of the trimmed MSA was calculated with PhyML 3.0 (56) on the Montpelier bioinformatics platform. The substitution model (LG + G + I) selection was made with SMS (57) using a Bayesian information criterion. The archaeal branch was used as an outgroup to root the ML tree. The joint reconstructions of all ancestral nodes were calculated on the GRASP (Graphical representation of ancestral sequence predictions) (58) web server using the Jones-Taylor-Thornton (JTT) evolutionary model.

The ThermoFisher GeneOptimizer tool was used to codon-optimize the amino acid sequences for cytosolic expression in *S. cerevisiae.* The subsequent DNA sequences were synthesized by GeneWiz in the pUC-GW-Kan vector and then assembled into the *RML2* ORF CRISPR backbone with 510 bp homology arms using Golden Gate assembly designed in Benchling. The assembled plasmids were transformed into *E. coli* dh5α and grown overnight on LB + 25 µg/mL chloramphenicol at 37 ºC. Non-fluorescent colonies were picked and grown overnight in liquid

LB + 25 µg/mL chloramphenicol and miniprepped using the Qiagen miniprep kit (Cat. No. / ID: 27104). Plasmid assembly was verified by sequencing (eurofins Genomics).

Growth Assays

To monitor the growth rate of the different strains, a colony was diluted in 200 µL H_2O. This mixture then went through a serial dilution of 30 µL in 170 µL of H_2O five times. 10 µL of each dilution was spotted on YPD and YPG (with the addition of antibiotics for the Cam^R and Ery^R experiments). Growth at 30 ºC was monitored over four days, and pictures were taken to observe colony size.

Flow cytometry

Three colonies were picked per strain and inoculated in YPD and grown overnight. The cultures were back-diluted 1:100 in 5 mL fresh YPD and harvested after 24 hours growth at 200 rpm for flow cytometry. The strains were further diluted 1:50 in 5mL fresh YPG and grown for a further 24 hours before harvesting for flow cytometry.

Samples were diluted 1:100 in 200 µL H_2O in a 96 well plate for flow cytometry. The samples were then run through a Cytoflex S flow cytometer with 10,000 samples recorded per well. The collected FITC, SSC and FSC data were analyzed using FlowJo, with doublets excluded via gating FSC-H plotted against FSC-A. The FITC values of the subsequent singlet populations were averaged per well to get fluorescence per cell values. Analysis was conducted in Prism9 using one-way or two-way ANOVAs with multiple comparisons, depending on the data. P-values are denoted with ns = $p > 0.05$, * = $p \leq 0.05$, ** = $p \leq 0.01$, *** = $p \leq 0.001$, *** = $p \leq 0.0001$.

Confocal Microscopy

Colonies were picked and grown overnight in 5mL YPG and then 1 mL of the culture was harvested by spinning at 13,000 rpm for 30 seconds. The supernatant was discarded and the pellet resuspended in 10-1000 µL H_2O? (depending on culture density). 2 µL of each sample was pipetted onto a microscope slide (Electron Microscopy Sciences 63422-06) that had been prepared with 1.4% agarose.

Images were acquired by Zeiss LSM 700 laser scanning confocal microscope using Plan-Apochromat 63x/1.4 Oil lens with pinhole size set to 1AU. Line average of 4 was applied. sfGFP image was captured in EGFP setting with 488nm lasers set to 50% intensity, 500 gain, and 1.58µs pixel dwell across the different samples. Post imaging adjustment was performed in Zen 2012 software (Zeiss).

Whole Genome Sequencing

Whole- genome sequencing was performed by Psomagen (Rockville, MD) using Illumina TruSeq DNA Nano 350 bp library prep and an Illumina NovaSeq 6000. Reads were aligned to the *S. cerevisiae* reference genome (yeastgenome.org) using the Burrows-Wheeler Aligner (59), Picard (http://broadinstitute.github.io/picard), SAMtools (60), and Genome Analysis Toolkit v3.8 (61). Variants were called against the reference genome using Mutect2 (61).

Physical interaction data was retrieved from BioGRID (34) for the proteins presenting mutations in mito-uL23$_{1-224}$ and suppressors 1 to 4. The physical interactions between mutated proteins and other proteins were visualized with CLANS (62).

References

1. Crick, F. (1970) Central Dogma of Molecular Biology. *Nature*, **227**, 561-563.

2. Bowman, J.C., Petrov, A.S., Frenkel-Pinter, M., Penev, P.I. and Williams, L.D. (2020) Root of the Tree: The Significance, Evolution, and Origins of the Ribosome. *Chem Rev*, **120**, 4848-4878.

3. Steitz, T.A. (2008) A Structural Understanding of the Dynamic Ribosome Machine. *Nat Rev Mol Cell Biol*, **9**, 242-253.

4. Krüger, A., Watkins, A.M., Wellington-Oguri, R., Romano, J., Kofman, C., DeFoe, A., Kim, Y., Anderson-Lee, J., Fisker, E. and Townley, J. (2023) Community Science Designed Ribosomes with Beneficial Phenotypes. *Nat Commun*, **14**, 961.

5. Kofman, C., Lee, J. and Jewett, M.C. (2021) Engineering Molecular Translation Systems. *Cell Systems*, **12**, 593-607.

6. de la Torre, D. and Chin, J.W. (2021) Reprogramming the Genetic Code. *Nat Rev Genet*, **22**, 169-184.

7. Bernier, C.R., Petrov, A.S., Kovacs, N.A., Penev, P.I. and Williams, L.D. (2018) Translation: The Universal Structural Core of Life. *Mol Biol Evol*, **35**, 2065-2076.

8. de Pouplana, L.R. (2020), *The Enzymes*. Elsevier, Vol. 48, pp. 11-37.

9. Koonin, E.V. (2003) Comparative Genomics, Minimal Gene-Sets and the Last Universal Common Ancestor. *Nat Rev Microbiol*, **1**, 127-136.

10. Hui, A. and De Boer, H.A. (1987) Specialized Ribosome System: Preferential Translation of a Single mRNA Species by a Subpopulation of Mutated Ribosomes in Escherichia coli. *Proc Natl Acad Sci USA*, **84**, 4762-4766.

11. Rackham, O. and Chin, J.W. (2005) A Network of Orthogonal Ribosome· mRNA Pairs. *Nat Chem Biol*, **1**, 159-166.

12. Schmied, W.H., Tnimov, Z., Uttamapinant, C., Rae, C.D., Fried, S.D. and Chin, J.W. (2018) Controlling Orthogonal Ribosome Subunit Interactions Enables Evolution of New Function. *Nature*, **564**, 444-448.

13. Orelle, C., Carlson, E.D., Szal, T., Florin, T., Jewett, M.C. and Mankin, A.S. (2015) Protein Synthesis by Ribosomes with Tethered Subunits. *Nature*, **524**, 119-124.

14. Chin, J.W. (2017) Expanding and Reprogramming the Genetic Code. *Nature*, **550**, 53-60.

15. Xie, J. and Schultz, P.G. (2005) Adding Amino Acids to the Genetic Repertoire. *Current Opin Chem Biol*, **9**, 548-554.

16. Roberts, G.G. and Hudson, A.P. (2006) Transcriptome Profiling of Saccharomyces Cerevisiae During a Transition from Fermentative to Glycerol-Based Respiratory Growth Reveals Extensive Metabolic and Structural Remodeling. *Mol Genet Genomics*, **276**, 170-186.

17. Turcotte, B., Liang, X.B., Robert, F. and Soontorngun, N. (2009) Transcriptional Regulation of Nonfermentable Carbon Utilization in Budding Yeast. *FEMS Yeast Res*, **10**, 2-13.

18. Käppeli, O. (1987) Regulation of Carbon Metabolism in Saccharomyces Cerevisiae and Related Yeasts. *Adv Microb Physiol*, **28**, 181-209.

19. Suhm, T., Habernig, L., Rzepka, M., Kaimal, J.M., Andréasson, C., Büttner, S. and Ott, M. (2018) A Novel System to Monitor Mitochondrial Translation in Yeast. *Microbial cell*, **5**, 158.

20. Weisblum, B. (1995) Erythromycin Resistance by Ribosome Modification. *Antimicrob Agents Chemother*, **39**, 577-585.

21. Clark-Walker, G. and Linnane, A.W. (1967) The Biogenesis of Mitochondria in Saccharomyces Cerevisiae: A Comparison between Cytoplasmic Respiratory-Deficient Mutant Yeast and Chloramphenicol-Inhibited Wild Type Cells. *J Cell Bio*, **34**, 1-14.

22. Dujon, B. (1980) Sequence of the Intron and Flanking Exons of the Mitochondrial 21s rRNA Gene of Yeast Strains Having Different Alleles at the Ω and Rib-1 Loci. *Cell*, **20**, 185-197.

23. Sor, F. and Fukuhara, H. (1982) Identification of Two Erythromycin Resistance Mutations in the Mitochondrial Gene Coding for the Large Ribosomal RNA in Yeast. *Nucleic Acids Res*, **10**, 6571-6577.

24. Desai, N., Brown, A., Amunts, A. and Ramakrishnan, V. (2017) The Structure of the Yeast Mitochondrial Ribosome. *Science*, **355**, 528-531.

25. Amunts, A., Brown, A., Bai, X.-c., Llácer, J.L., Hussain, T., Emsley, P., Long, F., Murshudov, G., Scheres, S.H. and Ramakrishnan, V. (2014) Structure of the Yeast Mitochondrial Large Ribosomal Subunit. *Science*, **343**, 1485-1489.

26. Petrov, A.S., Wood, E.C., Bernier, C.R., Norris, A.M., Brown, A. and Amunts, A. (2019) Structural Patching Fosters Divergence of Mitochondrial Ribosomes. *Mol Biol Evol*, **36**, 207-219.

27. Dragosits, M. and Mattanovich, D. (2013) Adaptive Laboratory Evolution–Principles and Applications for Biotechnology. *Microbial cell factories*, **12**, 1-17.

28. Ahn, M., Włodarski, T., Mitropoulou, A., Chan, S.H., Sidhu, H., Plessa, E., Becker, T.A., Budisa, N., Waudby, C.A. and Beckmann, R. (2022) Modulating Co-Translational Protein Folding by Rational Design and Ribosome Engineering. *Nat Commun*, **13**, 4243.

29. Jungfleisch, J., Nedialkova, D.D., Dotu, I., Sloan, K.E., Martinez-Bosch, N., Brüning, L., Raineri, E., Navarro, P., Bohnsack, M.T. and Leidel, S.A. (2017) A Novel Translational Control Mechanism Involving RNA Structures within Coding Sequences. *Genome Res*, **27**, 95-106.

30. Miller, J.E., Zhang, L., Jiang, H., Li, Y., Pugh, B.F. and Reese, J.C. (2018) Genome-Wide Mapping of Decay Factor–Mrna Interactions in Yeast Identifies Nutrient-Responsive Transcripts as Targets of the Deadenylase Ccr4. *G3: Genes, Genomes, Genetics*, **8**, 315-330.

31. Ho, Y., Gruhler, A., Heilbut, A., Bader, G.D., Moore, L., Adams, S.-L., Millar, A., Taylor, P., Bennett, K. and Boutilier, K. (2002) Systematic Identification of Protein Complexes in Saccharomyces Cerevisiae by Mass Spectrometry. *Nature*, **415**, 180-183.

32. Singh, A.P., Salvatori, R., Aftab, W., Aufschnaiter, A., Carlström, A., Forne, I., Imhof, A. and Ott, M. (2020) Molecular Connectivity of Mitochondrial Gene Expression and Oxphos Biogenesis. *Mol Cell*, **79**, 1051-1065. e1010.

33. Merz, S. and Westermann, B. (2009) Genome-Wide Deletion Mutant Analysis Reveals Genes Required for Respiratory Growth, Mitochondrial Genome Maintenance and Mitochondrial Protein Synthesis in Saccharomyces Cerevisiae. *Genome biology*, **10**, 1-18.

34. Oughtred, R., Chatr-aryamontri, A., Breitkreutz, B.-J., Chang, C.S., Rust, J.M., Theesfeld, C.L., Heinicke, S., Breitkreutz, A., Chen, D. and Hirschman, J. (2016) Biogrid: A Resource for Studying Biological Interactions in Yeast. *Cold Spring Harbor Protocols*, **2016**, pdb. top080754.

35. Lecompte, O., Ripp, R., Thierry, J.C., Moras, D. and Poch, O. (2002) Comparative Analysis of Ribosomal Proteins in Complete Genomes: An Example of Reductive Evolution at the Domain Scale. *Nucleic Acids Res*, **30**, 5382-5390.

36. Hug, L.A., Baker, B.J., Anantharaman, K., Brown, C.T., Probst, A.J., Castelle, C.J., Butterfield, C.N., Hernsdorf, A.W., Amano, Y. and Ise, K. (2016) A New View of the Tree of Life. *Nat Microbiol*, **1**, 1-6.

37. Gray, M.W. (1992) The Endosymbiont Hypothesis Revisited. *Int Rev Cytol*, **141**, 233-357.

38. Gray, M.W. (2015) Mosaic Nature of the Mitochondrial Proteome: Implications for the Origin and Evolution of Mitochondria. *Proc Natl Acad Sci USA*, **112**, 10133-10138.

39. Kummer, E. and Ban, N. (2021) Mechanisms and Regulation of Protein Synthesis in Mitochondria. *Nat Rev Mol Cell Biol*, **22**, 307-325.

40. Wysocki, R., Roganti, T., Van Dyck, E., de Derchove D'Exaerde, A. and Foury, F. (1999) Disruption and Basic Phenotypic Analysis of 18 Novel Genes from the Yeast Saccharomyces Cerevisiae. *Yeast*, **15**, 165-171.

41. Stenger, M., Le, D.T., Klecker, T. and Westermann, B. (2020) Systematic Analysis of Nuclear Gene Function in Respiratory Growth and Expression of the Mitochondrial Genome in S. Cerevisiae. *Microbial cell*, **7**, 234.

42. Bonnefoy, N. and Fox, T.D. (2007) Directed Alteration of Saccharomyces Cerevisiae Mitochondrial DNA by Biolistic Transformation and Homologous Recombination. *Mitochondria: Practical Protocols*, 153-166.

43. Mi, L., Shi, M., Li, Y.-X., Xie, G., Rao, X., Wu, D., Cheng, A., Niu, M., Xu, F. and Yu, Y. (2023) Ddda Homolog Search and Engineering Expand Sequence Compatibility of Mitochondrial Base Editing. *Nat Commun*, **14**, 874.

44. Myers, A.M., Pape, L.K. and Tzagoloff, A. (1985) Mitochondrial Protein Synthesis Is Required for Maintenance of Intact Mitochondrial Genomes in Saccharomyces Cerevisiae. *EMBO J*, **4**, 2087-2092.

45. Lecrenier, N. and Foury, F. (1995) Overexpression of the Rnr1 Gene Rescues Saccharomyces Cerevisiae Mutants in the Mitochondrial DNA Polymerase-Encoding Mip1 Gene. *Molecular and General Genetics MGG*, **249**, 1-7.

46. Grasso, K.T., Singha Roy, S.J., Osgood, A.O., Yeo, M.J.R., Soni, C., Hillenbrand, C.M., Ficaretta, E.D. and Chatterjee, A. (2022) A Facile Platform to Engineer Escherichia coli Tyrosyl-tRNA Synthetase Adds New Chemistries to the Eukaryotic Genetic Code, Including a Phosphotyrosine Mimic. *ACS central science*, **8**, 483-492.

47. Bonitz, S.G., Berlani, R., Coruzzi, G., Li, M., Macino, G., Nobrega, F.G., Nobrega, M.P., Thalenfeld, B.E. and Tzagoloff, A. (1980) Codon Recognition Rules in Yeast Mitochondria. *Proc Natl Acad Sci USA*, **77**, 3167-3170.

48. Katoh, T., Tajima, K. and Suga, H. (2017) Consecutive Elongation of D-Amino Acids in Translation. *Cell Chem Biol*, **24**, 46-54.

49. Englander, M.T., Avins, J.L., Fleisher, R.C., Liu, B., Effraim, P.R., Wang, J., Schulten, K., Leyh, T.S., Gonzalez Jr, R.L. and Cornish, V.W. (2015) The Ribosome Can Discriminate the Chirality of Amino Acids within Its Peptidyl-Transferase Center. *Proc Natl Acad Sci USA*, **112**, 6038-6043.

50. O'donoghue, P., Ling, J., Wang, Y.-S. and Söll, D. (2013) Upgrading Protein Synthesis for Synthetic Biology. *Nat Chem Biol*, **9**, 594-598.

51. Espinosa, M.I., Gonzalez-Garcia, R.A., Valgepea, K., Plan, M.R., Scott, C., Pretorius, I.S., Marcellin, E., Paulsen, I.T. and Williams, T.C. (2020) Adaptive Laboratory Evolution of Native Methanol Assimilation in Saccharomyces Cerevisiae. *Nat Commun*, **11**, 1-12.

52. Penev, P.I., McCann, H.M., Meade, C.D., Alvarez-Carreno, C., Maddala, A., Bernier, C.R., Chivukula, V.L., Ahmad, M., Gulen, B. and Sharma, A. (2021) Proteovision: Web Server for Advanced Visualization of Ribosomal Proteins. *Nucleic Acids Res*, **49**, W578-W588.

53. Valach, M., Gonzalez Alcazar, J.A., Sarrasin, M., Lang, B.F., Gray, M.W. and Burger, G. (2021) An Unexpectedly Complex Mitoribosome in Andalucia Godoyi, a Protist with the Most Bacteria-Like Mitochondrial Genome. *Mol Biol Evol*, **38**, 788-804.

54. Katoh, K. and Toh, H. (2010) Parallelization of the MAFFT Multiple Sequence Alignment Program. *Bioinformatics*, **26**, 1899-1900.

55. Morrison, D.A. and Ellis, J.T. (1997) Effects of Nucleotide Sequence Alignment on Phylogeny Estimation: A Case Study of 18S Rdnas of Apicomplexa. *Mol Biol Evol*, **14**, 428-441.

56. Elías-Román, R., Guzmán-Plazola, R., Klopfenstein, N., Alvarado-Rosales, D., Calderón-Zavala, G., Mora-Aguilera, J., Kim, M.S. and García-Espinosa, R. (2013) Incidence and Phylogenetic Analyses of a Rmillaria Spp. Associated with Root Disease in Peach Orchards in the State of M Exico, M Exico. *For Pathol*, **43**, 390-401.

57. Lefort, V., Longueville, J.-E. and Gascuel, O. (2017) Sms: Smart Model Selection in Phyml. *Mol Biol Evol*, **34**, 2422-2424.

58. Ross, C.M., Foley, G., Boden, M. and Gillam, E.M. (2022) Using the Evolutionary History of Proteins to Engineer Insertion-Deletion Mutants from Robust, Ancestral Templates Using Graphical Representation of Ancestral Sequence Predictions (Grasp). *Enzyme engineering: methods and protocols*, 85-110.

59. Li, H. and Durbin, R. (2009) Fast and Accurate Short Read Alignment with Burrows–Wheeler Transform. *Bioinformatics*, **25**, 1754-1760.

60. Li, H., Handsaker, B., Wysoker, A., Fennell, T., Ruan, J., Homer, N., Marth, G., Abecasis, G., Durbin, R. and Subgroup, G.P.D.P. (2009) The Sequence Alignment/Map Format and Samtools. *Bioinformatics*, **25**, 2078-2079.

61. Van der Auwera, G.A. and O'Connor, B.D. (2020) *Genomics in the Cloud: Using Docker, Gatk, and Wdl in Terra*. O'Reilly Media.

62. Frickey, T. and Lupas, A. (2004) Clans: A Java Application for Visualizing Protein Families Based on Pairwise Similarity. *Bioinformatics*, **20**, 3702-3704.